Spatiotemporal deformations of reflectionless potentials

S. A. R. Horsley*
Department of Physics and Astronomy, University of Exeter, Stocker Road, Exeter EX4 4QL, United Kingdom

S. Longhi†
Dipartimento di Fisica, Politecnico di Milano and Istituto di Fotonica e Nanotecnologie del Consiglio Nazionale delle Ricerche, Piazza L. da Vinci 32, 20133 Milano, Italy

(Received 3 April 2017; published 17 August 2017)

Reflectionless potentials for classical or matter waves represent an important class of scatteringless systems encountered in different areas of physics. Here we mathematically demonstrate that there is a family of non-Hermitian potentials that, in contrast to their Hermitian counterparts, remain reflectionless even when deformed in space or time. These are the profiles that satisfy the spatial Kramers-Kronig relations. We start by considering scattering of matter waves for the Schrödinger equation with an external field, where a moving potential is observed in the Kramers-Henneberger reference frame. We then generalize this result to the case of electromagnetic waves, by considering a slab of reflectionless material that both is scaled and has its center displaced as an arbitrary function of position. We analytically and numerically demonstrate that the backscattering from these profiles remains zero, even for extreme deformations. Our results indicate the supremacy of non-Hermitian Kramers-Kronig potentials over reflectionless Hermitian potentials in keeping their reflectionless property under deformation and could find applications to, e.g., reflectionless optical coatings of highly deformed surfaces based on perfect absorption.

DOI: 10.1103/PhysRevA.96.023841

I. INTRODUCTION

In classical mechanics, a spatially varying potential $V(\boldsymbol{x})$ causes a particle to accelerate with a force $-\nabla V(\boldsymbol{x})$. In quantum mechanics the particle is replaced by a wave and the spatial variation of the potential not only causes a wave packet to accelerate, but also generates reflection. Typically, the more rapid the change of the potential the more reflection there is. Yet there are some spatial variations of the potential that do not lead to any reflection at all. The most interesting of these are potentials that vary rapidly in space (compared to the wavelength) and remain reflectionless for all particle energies.

The known reflectionless potentials can be divided into two broad classes: Hermitian and non-Hermitian. The reflectionless Hermitian potentials are real valued and include well-known examples such as the Pöschl-Teller and Kay-Moses potentials [1–3], which can be related to inverse scattering theory [4], the solitons of the Kortweg–de Vries equation [5], and the theory of supersymmetric quantum mechanics [6]. It is worth mentioning that while the Pöschl-Teller potential has been a theoretical curiosity for a long time, it has a natural physical realization in magnetism: Exchange spin waves (which obey a Schrödinger-like equation) do not reflect from domain walls because the effect of the domain wall is equivalent to that of a Pöschl-Teller potential (see, e.g., [7]).

In contrast, the reflectionless non-Hermitian potentials contain regions of space where the wave is dissipated or amplified. In quantum physics, non-Hermitian (complex) potentials generally arise in effective Hamiltonian descriptions of open quantum systems [8] or in parity-time ($\mathcal{PT}$) -symmetric extensions of quantum mechanics [9,10]. Such potentials also have an equivalent in any wave theory, most of which are not restricted to be Hermitian. For example, a complex reflectionless potential $V(x)$ in quantum physics is equivalent to a complex-valued graded permittivity profile $\epsilon(x)$ in optics that does not reflect electromagnetic waves (for one or both polarizations), whatever the angle of incidence. In optics, a complex permittivity profile $\epsilon(x)$ simply describes a dielectric medium possessing spatial regions with optical gain and loss. In particular, the class of $\mathcal{PT}$-symmetric non-Hermitian potentials have attracted great interest in recent years. This largely originates from the work of Bender and Boettcher [9,10], who showed that operators with real spectra are not necessarily Hermitian. $\mathcal{PT}$-symmetric potentials have since been translated into optics and acoustics where it has been realized that such potentials can be perfectly transparent for waves incident from one side [11–16], an effect that has been confirmed in recent experiments [16–19].

Another class of reflectionless non-Hermitian potentials are those that satisfy the spatial Kramers-Kronig relations [20–23] (see also the work of Milton [24] on analytic materials). These complex potentials do not reflect waves incident from one side of the potential, independent of parameters such as the energy (in quantum mechanics), or angle of incidence and frequency (in optics or acoustics). Similar behavior was anticipated by Berry [25] and Milton [26] in their analysis of wave propagation through periodic media, but more generally comprise an enormous family of reflectionless, invisible [21,22], and even bidirectionally invisible [27] potentials. One of these profiles was recently experimentally realized by Jiang *et al.* [28], mapping the frequency response of a metamaterial structure onto space, converting the frequency domain Kramers-Kronig relations into spatial ones.

In this work we are concerned with the question of whether reflectionless potentials remain reflectionless even when they

*s.horsley@exeter.ac.uk
†stefano.longhi@polimi.it

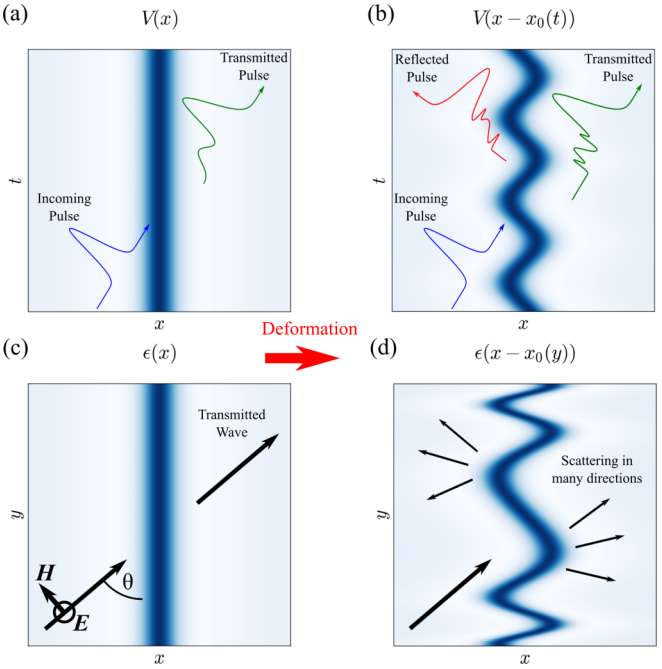

FIG. 1. Schematic of the two cases considered in this work. (a) and (b) Typical wave-packet scattering from a moving potential $V(x - x_0(t))$ that is reflectionless when stationary. At initial time $t = 0$ the wave packet is localized on the far left of the scattering potential and propagates in the forward direction with a group velocity v_g. In most cases the motion of the potential leads to a reflected pulse. (c) and (d) Plane wave (here shown as TE polarized) incident on a reflectionless graded slab of permittivity $\epsilon(x)$. If the slab is deformed through displacing its center as a function of y, $\epsilon(x) \to \epsilon(x - x_0(y))$, then this typically causes the reflection and transmission to be much more complicated.

are deformed in space or time (cf. Fig. 1). The main result of our study is that, while Hermitian potentials of Pöschl-Teller or Kay-Moses type lose their reflectionless property when deformed, non-Hermitian Kramers-Kronig potentials remain one-way reflectionless under a broad class of deformations in space or time. Such a result indicates the supremacy of non-Hermitian reflectionless potentials over Hermitian ones, paving the way toward the synthesis of a novel class of reflectionless structures. Specifically, we consider the case of a moving reflectionless potential for matter waves within a complex extension of the Schrödinger equation (motion can be thought of as a deformation over time) and spatial deformation of a reflectionless dielectric slab for electromagnetic waves.

II. SCATTERING OF MATTER WAVES FROM A MOVING POTENTIAL

As the first example of reflectionless deformed potentials we consider the scattering of matter waves from a moving one-dimensional potential $V(x)$ (see Fig. 1). The Schrödinger equation describing the temporal evolution of the amplitude probability $\psi(x,t)$ of matter waves reads

$$i\hbar\frac{\partial\psi(x,t)}{\partial t} = \left[-\frac{\hbar^2}{2m}\frac{\partial^2}{\partial x^2} + V(x - x_0(t))\right]\psi(x,t), \qquad (1)$$

where $x_0(t)$ is a rather arbitrary real-valued function of time t that describes the motion of the potential and $V(x) \to 0$ as $|x| \to \pm\infty$. We note that in ordinary nonrelativistic quantum mechanics a moving quantum potential is found, for example, in laser-atom physics when an atom interacts with an intense and high-frequency laser field [29–32] or in matter wave systems when ultracold atoms are trapped in a moving optical potential realized by interference of chirped laser fields [33]. In the former case the Schrödinger equation (1) with a moving potential describes the electron dynamics in the Kramers-Henneberger reference frame [29,32], the rest frame of a classical electron in the laser field, where the atomic core appears to oscillate at the frequency of the driving laser field and $x_0(t)$ describes the quiver motion of the electron solely under the action of the external laser field. In fact, let us consider the moving atom reference frame

$$x' = x - x_0(t), \quad t' = t, \qquad (2)$$

where the potential (i.e., the atom) is at rest. We now apply a gauge transformation to transform the Schrödinger equation into this noninertial reference frame (see, e.g., [34])

$$\phi(x',t') = \psi(x',t')\exp\left[-i\frac{m\dot{x}_0}{\hbar}x' - i\frac{m}{2\hbar}\int_0^{t'} d\xi\,\dot{x}_0^2(\xi)\right] \qquad (3)$$

(where the overdot indicates the derivative with respect to time); the evolution equation for the amplitude probability $\phi(x',t')$ reads

$$i\hbar\frac{\partial\phi(x',t')}{\partial t'} = \left[-\frac{\hbar^2}{2m}\frac{\partial^2}{\partial x'^2} + V(x') - F(t')x'\right]\phi(x',t'), \qquad (4)$$

where $F(t') \equiv -m\ddot{x}_0(t')$. In the (x',t') reference frame, in addition to the stationary force $-(dV/dx')$ the electron experiences the additional noninertial force $F(t')$, which physically describes the dipole interaction with an external electric field $\mathcal{E}(t') = -F(t')/e = (m/e)\ddot{x}_0(t')$.

Owing to the Galilean invariance of the Schrödinger equation, the scattering and localization properties of a uniformly moving potential $x_0(t) = vt$ are clearly the same as those of the static (at rest) potential because the force $F(t')$ vanishes. Hence, if $V(x)$ belongs to the class of reflectionless potentials, the uniformly moving potential remains reflectionless. However, for an accelerated motion this is not the case. For example, taking an oscillating trajectory $x_0(t) = A\cos(\omega t)$ at high frequency $\omega = 2\pi/T$, an application of Floquet theory shows that to leading order the moving potential can be replaced by its time-average static potential $V_{av}(x) = (1/T)\int_0^T dt\, V(x - x_0(t))$. Since $V_{av}(x)$ is generally different from $V(x)$, the scattering and localization properties of the static and rapidly oscillating potentials are thus rather different. For Hermitian potentials, Floquet theory explains important physical effects such as adiabatic stabilization in strong-field atomic physics [29–32,35] and field-induced barrier transparency in resonant quantum tunneling [36,37]. Note that if $V(x)$ belongs the class of reflectionless potentials, $V_{av}(x)$ generally does not, so the reflectionless feature of the potential is generally lost when it rapidly oscillates in time. This is the case, for example, when the Pöschl-Teller potentials are oscillated in time (see Fig. 2). Conversely, if $V(x)$ is a Kramers-Kronig reflectionless potential, i.e., if $V(x)$ is an analytic function in the half

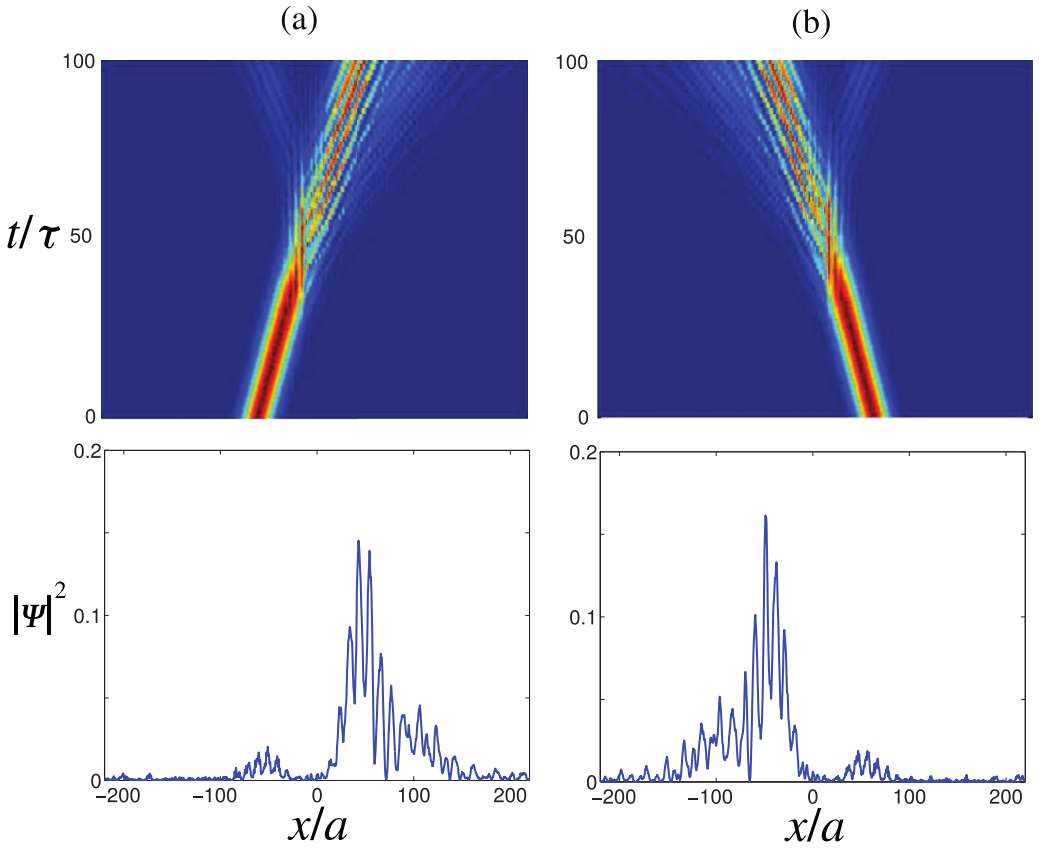

FIG. 2. Wave packet scattering, for (a) left and (b) right incidence sides, from an oscillating Pöschl-Teller potential $V(x - x_0(t))$, with $V(x) = -2/\cosh^2(x/a)$, $x_0(t) = 10\cos(t/\tau)$, $\hbar = 1$, and $m = 1$. At initial time $t = 0$ the wave packet is a Gaussian distribution localized far from the scattering potential and propagates with a group velocity $v_g = 1$. The top panels show the temporal evolution of the probability distribution $|\psi(x,t)|^2$ on a pseudocolor map, whereas the bottom panels depict the probability distribution $|\psi(x,t)|^2$ at time $t = 100\tau$.

complex plane $\mathrm{Im}(x) \geqslant 0$, then it readily follows that $V_{av}(x)$ is a Kramers-Kronig potential as well, i.e., in this case the reflectionless property of the potential is not lost. We wish now to prove that a Kramers-Kronig potential remains one-way reflectionless for an arbitrary trajectory $x_0(t)$. To this aim, let us expand the wave function $\psi(x,t)$ as a superposition of plane waves (momentum representation)

$$\psi(x,t) = \int_{-\infty}^{\infty} dk\, c(k,t) \exp[ikx - i\omega(k)t], \tag{5}$$

where k is the wave number and $\omega(k) = \hbar k^2/2m$ (the dispersion relation of the free particle). Let us assume that $V(x)$ admits the Fourier decomposition

$$V(x) = \int_{-\infty}^{\infty} dk\, \hat{V}(k) \exp(ikx), \tag{6}$$

with the Fourier spectrum $\hat{V}(k) = (1/2\pi) \int dx\, V(x) \exp(-ikx)$. Substitution of the ansatz (5) into Eq. (1) yields the following integro-differential equation for $c(k,t)$:

$$i\hbar \frac{\partial c(k,t)}{\partial t} = \int_{-\infty}^{\infty} dq\, \hat{V}(q) c(k-q,t) \times \exp[i\omega(k)t - i\omega(k-q)t - iqx_0(t)]. \tag{7}$$

The scattering problem for an arbitrarily moving potential should be stated in terms of time-dependent inelastic scattering theory; however, for our purposes it is more convenient to formulate the scattering problem in terms of wave packets (Fig. 1) using Eq. (7) in momentum representation to study the wave evolution. At initial time $t = 0$ we assume that $\psi(x,0)$ describes a wave packet, localized far from the scattering potential on the far left side, with carrier wave number $k = k_0$, so that $c(k,0)$ is a narrow function of k at around $k = k_0$ (see Fig. 1). Far from the scattering potential, the wave packet moves from the left to the right side with a group velocity $v_g = (d\omega/dk)_{k_0} = \hbar k_0/m$. Let us also assume that the incident wave packet is composed by only positive wave numbers (progressive waves), i.e., $c(k,0) = 0$ for $k \leqslant 0$. Then, for any Kramers-Kronig potential, i.e., provided $V(x)$ is holomorphic in the $\mathrm{Im}(x) \geqslant 0$ half complex plane, the moving potential is reflectionless for left incidence side. In fact, for Kramers-Kronig potentials one has $\hat{V}(q) = 0$ for $q < 0$, and from Eq. (7) it follows that the derivative of $c(k,t)$ in time depends only on the values of $c(\xi,t)$ for $\xi \leqslant 0$. Since $c(k,0) = 0$ for any $k \leqslant 0$, it follows that $c(k,t) = 0$ for $k \leqslant 0$ at any arbitrary time $t > 0$. This means that, at any time t, the wave-packet spectrum $c(k,t)$ is composed by only positive spatial wave numbers k and thus it cannot give rise to any reflected wave packet (this would obviously require excitation of negative-wave-number components). An

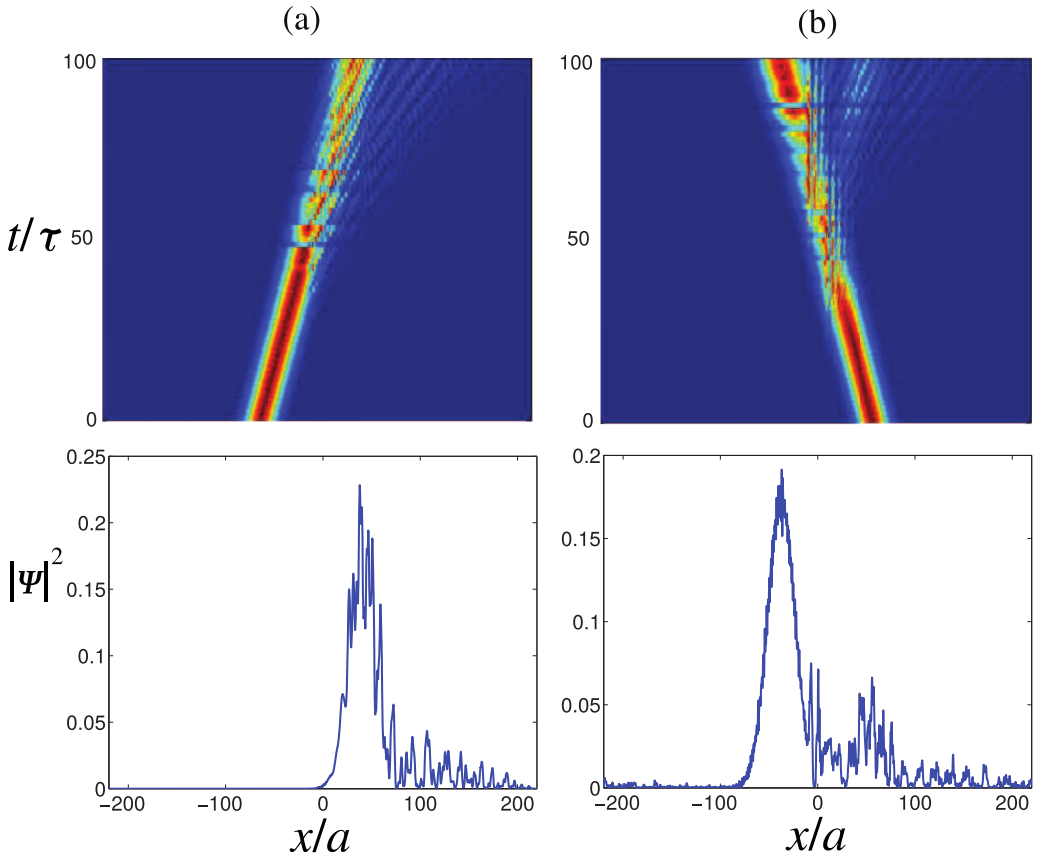

FIG. 3. Same as in Fig. 2 [the moving potential is oscillatory $x_0(t) = A\cos(t/\tau)$, with $A = 10$], but for the Kramers-Kronig potential $V(x) = -1/(x/a + i)^2$.

example of a one-way reflectionless Kramers-Kronig moving potential, corresponding to an oscillatory trajectory $x_0(t) = A\cos(\omega t)$, is shown in Fig. 3.

III. SCATTERING OF ELECTROMAGNETIC WAVES FROM A DEFORMED DIELECTRIC SLAB

There is a close relationship between the evolution of a Schrödinger wave in a moving potential $V(x - x_0(t))$ and the behavior of an electromagnetic wave incident onto a graded permittivity with a smoothly displaced center $\epsilon(x - x_0(y))$ (as shown in Fig. 1) [37]. To see this analogy directly, consider the wave equation for the electric field E_z of TE-polarized radiation propagating in the x-y plane

$$\left[\frac{\partial^2}{\partial x^2} + \frac{\partial^2}{\partial y^2} + k_0^2\epsilon(x - x_0(y))\right]E_z(x,y) = 0, \qquad (8)$$

where $k_0 = \omega/c$ is the free-space wave number. If the y dependence of the profile is very slow in space then we can write the electric field as a function of two scales $E_z(x,y) \to E_z(x,y',y'')$, where $y' = k_0 y$ is associated with the oscillation of the wave and $y'' = y/a$ with the scale over which the profile is deformed significantly. Introducing these two scales into (8), one finds, to leading order in $1/a$,

$$\left[-\frac{1}{2k_0^2}\frac{\partial^2}{\partial x^2} + \frac{1}{2}[1 - \epsilon(x - x_0(y''))]\right]\varphi = \frac{i}{k_0 a}\frac{\partial \varphi}{\partial y''}, \qquad (9)$$

where $E_z(x,y',y'') = \exp(iy')\varphi(x,y'')$. Equation (9) is of the same form as the Schrödinger equation in a time-dependent potential (1), with the time evolution of the potential V being equivalent to the slow change of $1 - \epsilon$ along the y axis. Therefore, all results given in Sec. II hold for monochromatic electromagnetic waves close to grazing incidence onto a slowly deformed slab of graded material. In particular, complex profiles satisfying the spatial Kramers-Kronig relations will remain reflectionless from one side, even if they are slowly deformed.

In the context of optics this result is far less surprising than in quantum mechanics. In contrast to our exact results for the Schrödinger equation, Eq. (9) is valid only when $k_0 a \ll 1$. This is equivalent to an adiabatic approximation, where the potential is changed much more slowly than the oscillation of the wave. In such an adiabatic regime we would not in any case have expected the spatial dependence of the potential to generate any additional reflection. The obvious question is whether a *nonadiabatic* deformation of a Kramers-Kronig potential generates any reflection.

Given the z invariance of our system, we can decompose our electromagnetic field into TE and TM polarizations, with E_z and H_z obeying, respectively, the equations

$$\nabla^2 E_z + k_0^2\epsilon(x - x_0(y))E_z = 0,$$
$$\nabla \cdot \frac{1}{\epsilon(x - x_0(y))}\nabla H_z + k_0^2 H_z = 0. \qquad (10)$$

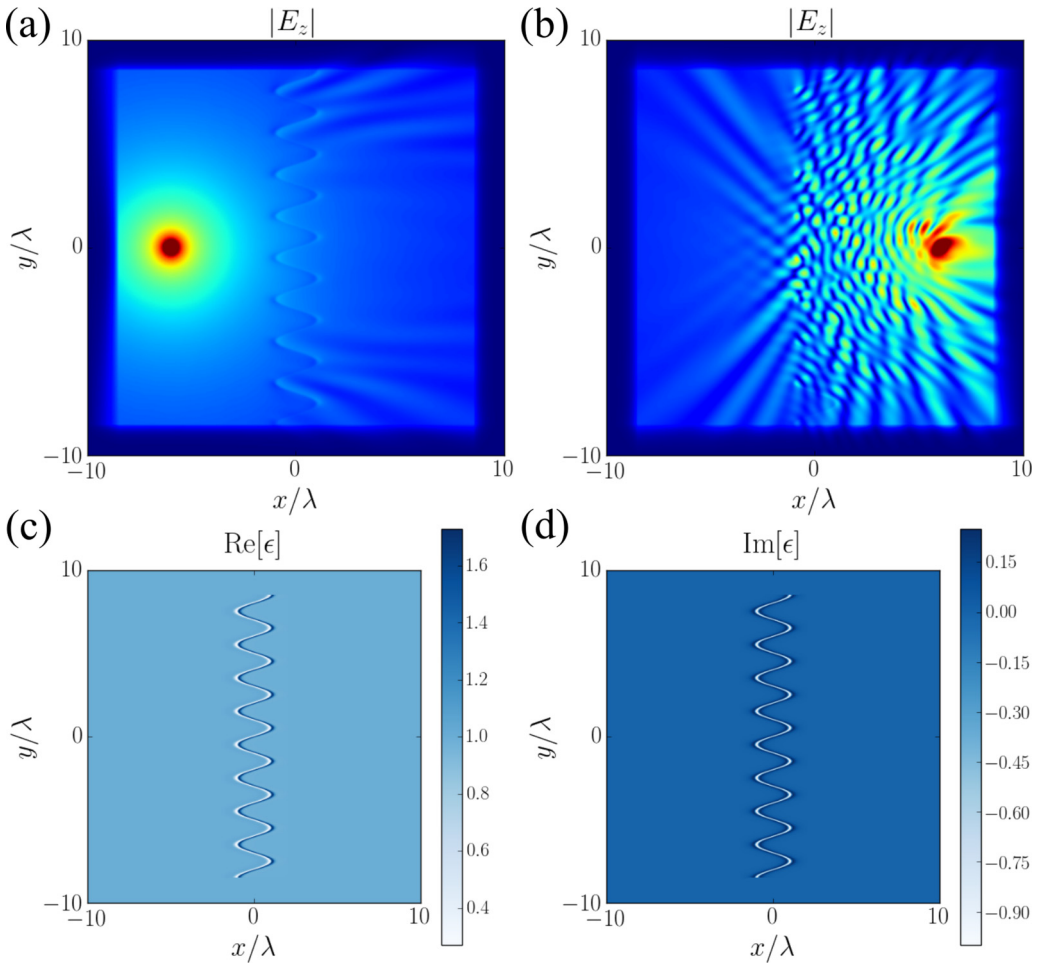

FIG. 4. A source of TE-polarized radiation is situated away from a deformed slab of a Kramers-Kronig medium, designed to be reflectionless from the left $\epsilon(x,y) = 1 - a/[x - x_0(y) + ia]^3$, where $a = \lambda/5$ and $x_0(y) = \lambda \sin(\pi y/\lambda)$. The numerically calculated (COMSOL multiphysics) time-averaged field of a source is shown (a) on the left of the medium $x = -6\lambda$ and (b) on the right $x = 6\lambda$. Also shown are the (c) real and (d) imaginary parts of the permittivity of the deformed profile.

By construction, the function $\epsilon(x)$ is analytic in the upper half complex position plane and thus can be written as

$$\epsilon(x) = 1 + \int_0^\infty \frac{dk}{2\pi} \tilde{\epsilon}(k) e^{ikx}. \tag{11}$$

Assuming it is also free of zeros (if it is not then our results apply only for TE polarization), we can continuously displace both of Eqs. (10) from the real line to $x' = x_1 + ix_2$, where the fixed value of x_2 is positive and very large. On this line the permittivity is very close to unity and very slowly changing with position [i.e., the value of the integral (11) decreases in magnitude, with the higher Fourier components being heavily damped out]. The adiabatic approximation will therefore become arbitrarily accurate on the whole of this line with increasing x_2 and the reflection from the profile must becomes vanishingly small (see [22] for a more detailed discussion). However, if we return to the real line $x_2 = 0$ and consider waves incident from the left of this profile we know in general that on the far left $x_1 \to -\infty$ we have incident plus scattered waves, e.g.,

$$E_z(x,y) \sim e^{i(k_x x + k_y y)} + \int_{-\infty}^{\infty} \frac{dK_y}{2\pi} r(K_y,k_y) e^{-i\sqrt{k_0^2 - K_y^2}x} e^{iK_y y'}, \tag{12}$$

where $r(K_y,k_y)$ is the scattering coefficient, coupling different angles of propagation through the deformed profile $\epsilon(x - x_0(y))$. If we displace this result from the real line up to the same large value of x_2 then we see that the second term in (12) becomes exponentially large, swamping the incident field. This contradicts the behavior we predicted, where the reflection ought to *vanish* with increasing x_2. The only resolution to this paradox is if the scattering is exactly zero on the real line, in which case it is also zero throughout the upper half position plane. A permittivity profile obeying the spatial Kramers-Kronig relations must therefore remain reflectionless from one side, even if it is deformed through an arbitrary y-dependent displacement of its center. Figures 4 and 5 show a numerical demonstration of this result.

Through consideration of the above analyticity argument, it is also evident that other kinds of deformation can be applied without inducing any reflection. We now consider a family of deformations obtained through replacing the argument of the planar permittivity profile x with a new function $X(x,y)$, the planar profile becoming a function of both x and y. These deformations must be such that the introduction of the y dependence $\epsilon(X) = \epsilon(X(x,y))$ does not change the analyticity

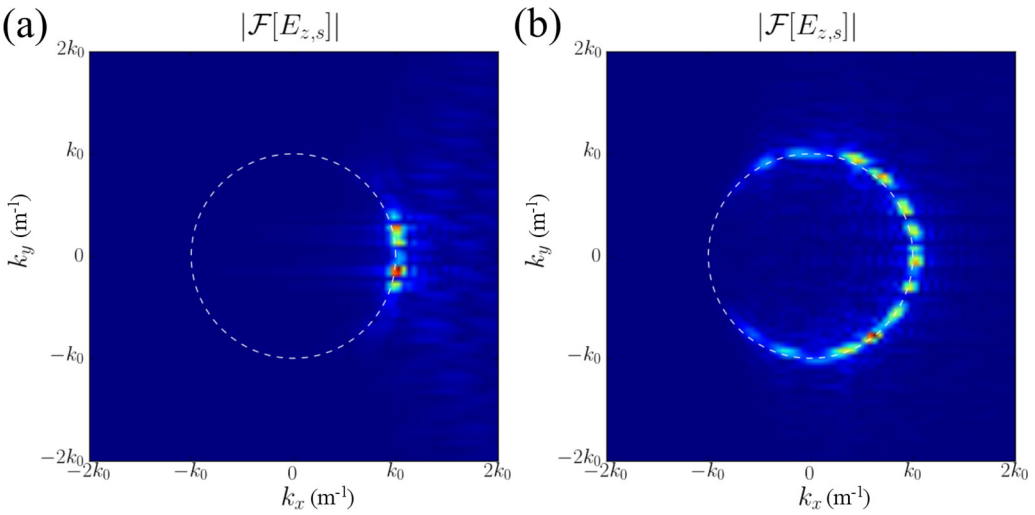

FIG. 5. Fourier magnitude of the scattered part of the electric field $E_{z,s} = E_z - E_{z,0}$ ($E_{z,0}$ is the field of the line source in an empty simulation domain) corresponding to (a) Fig. 4(a), showing no backscattering from the slab, and (b) Fig. 4(b), illustrating very strong backscattering and weak forward scattering.

of the permittivity in the upper half plane of the complex variable x. In other words, the function $X(x,y)$ must be a conformal map depending on the parameter y, but always mapping the upper half x plane to the upper half X plane, with $\mathrm{Im}[X] \to \infty$ as $x_2 \to \infty$.

Our procedure for finding such a family of functions X is illustrated in Fig. 6. We first use a Möbius transformation to map the upper half x plane to the unit disk of the w plane [38]

$$w(x) = \frac{x-i}{x+i}, \quad x(w) = i\left(\frac{1+w}{1-w}\right), \tag{13}$$

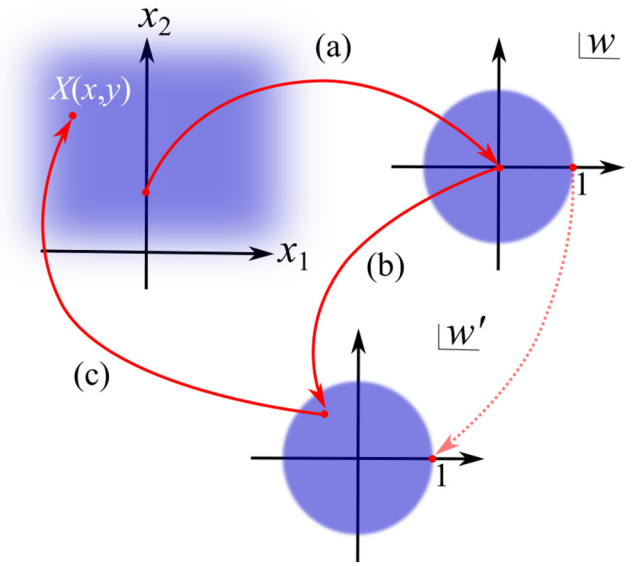

FIG. 6. Schematic of the sequence of conformal transformations applied to obtain the deformation function $X(x,y)$ (15). (a) The upper half complex position plane is first mapped onto the unit disk ($x_2 \to \infty$ being mapped into the region close to $w = 1$). (b) A second transformation then moves around the points on the unit disk in a way that is dependent on the y coordinate, while keeping the point $w = 1$ fixed. (c) Finally, the unit disk is mapped back to the upper half complex position plane.

where $x_2 \to \infty$ is mapped to the vicinity of $w = 1$. We now perform a second transformation $w \to w'$ that maps the unit circle to itself, keeping the point $w = 1$ fixed [39]

$$w'(x,y) = e^{i\phi}\left(\frac{w^n(x) - \eta(y)}{\eta^\star(y) w^n(x) - 1}\right), \tag{14}$$

where n is a positive integer, $\phi = \pi - 2\arg[\eta - 1]$, and the arbitrary function $\eta(y)$ has a modulus less than unity $|\eta(y)| < 1$. Performing the inverse map given in (13) then yields the desired family of deformations that can be applied to the potential while keeping it reflectionless from one side:

$$X(x,y) = \left(\frac{i}{1-|\eta|^2}\right) \times \frac{[2\eta^\star - 1 - |\eta|^2](x-i)^n + [2\eta - 1 - |\eta|^2](x+i)^n}{(x-i)^n - (x+i)^n}. \tag{15}$$

For the case where $n = 1$, this rather complicated x and y dependence reduces to a simple scaling and displacement of the profile

$$X(x,y) = \frac{|1-\eta(y)|^2}{1-|\eta(y)|^2} x + \frac{2\,\mathrm{Im}[\eta(y)]}{1-|\eta(y)|^2} = \frac{1}{\sigma(y)}[x - x_0(y)] \quad \text{for } n = 1, \tag{16}$$

demonstrating that we not only can displace the profile as an arbitrary function of y, but at the same time can squash and stretch it without introducing any reflection. The more complicated cases of $n = 2,3$ reveals the general pattern in (15),

$$X(x,y) = \begin{cases} \frac{1}{\sigma(y)}\left[\left(x - \frac{1}{x}\right) - x_0(y)\right], & n = 2 \\ \frac{1}{\sigma(y)}\left[\left(\frac{x^3 - 3x}{3x^2 - 1}\right) - x_0(y)\right], & n = 3. \end{cases} \tag{17}$$

These are again y-dependent displacements plus scaling, but in both cases the variable x has been replaced with

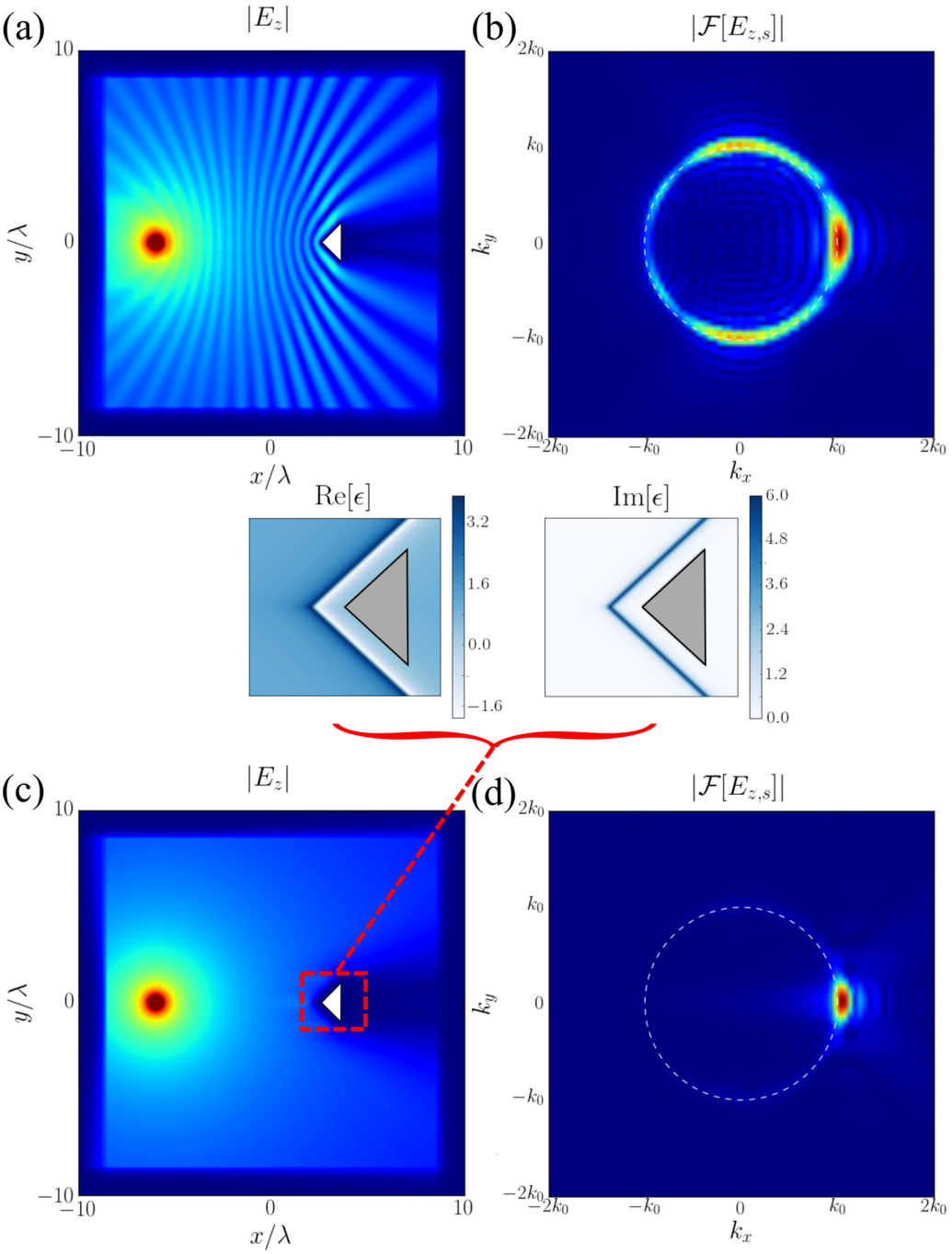

FIG. 7. (a) A metal wedge of a size on the order of the wavelength strongly scatters electromagnetic radiation. (b) The Fourier transform of the scattered field (defined as in Fig. 5) shows scattering in all directions, with the strong forward scattering evident due to the shadow behind the object. (c) and (d) Covering the metal wedge in the deformed analytic profile shown in the subpanels removes all the backscattering. In this case the profile is entirely lossy for $\epsilon(X) = 1 - 1/(X/a + i)$, with $a = \lambda/20$ and $X(x,y)$ defined as in (16) with $x_0(y) = 2\lambda + |y|$ and $\sigma(y) = \frac{1}{4}[1 - \mathrm{sgn}(y - y_c)][1 + \mathrm{sgn}(y + y_c)]$ ($y_c = 3\lambda/2$).

a function that returns a complex number in the upper half plane when x is in the upper half plane. The same behavior is evident for all n, with X having the general form $X(x,y) = \sigma(y)[x'(x) - x_0(y)]$, where $x'(x)$ is a conformal map of the upper half position plane to itself. Figure 7 demonstrates an example of a combined scaling and displacement operation, applied to design an absorbing coating that removes the scattering from a metallic wedge. We note that the above analysis may explain why the Kramers-Kronig relations function so well as absorbing coatings on sharp corners, as shown in the numerical simulations of [28].

As a final comment, we analyze the wave scattering problem of a deformed slab for the Helmholtz equation (8) through employing a coordinate transformation, similar to the Kramers-Henneberger reference frame transformation for the Schrödinger equation, that makes the dielectric profile flat.

For example,

$$x' = \frac{1}{\sigma(y)}[x - x_0(y)], \quad x = \sigma(y')x' + x_0(y'),$$
$$y' = y, \quad y = y' \tag{18}$$

deform the profiles discussed above to ordinary planar ones $\epsilon(x')$. As is well established in the theory of transformation optics [40,41], such a coordinate transformation is equivalent to the introduction of an inhomogeneous anisotropic medium into the x'-y' coordinate system; i.e., the deformed slab in empty space has the same influence on electromagnetic waves as a flat slab embedded in a material. Assuming that the x-y coordinate system contains the profile $\epsilon(x,y)$, the equivalent medium in the x'-y' coordinate system (18) has in-plane relative permeability and permittivity equal to

$$\boldsymbol{\epsilon}(x',y') = \epsilon(x')\sqrt{g}\boldsymbol{g}^{-1}$$
$$= \frac{\epsilon(x')}{\sigma}\begin{pmatrix} 1+(\dot\sigma x'+\dot x_0)^2 & -\sigma(\dot\sigma x'+\dot x_0) \\ -\sigma(\dot\sigma x'+\dot x_0) & \sigma^2 \end{pmatrix},$$
$$\boldsymbol{\mu}(x',y') = \sqrt{g}\boldsymbol{g}^{-1}, \tag{19}$$

where $\dot x_0 = \partial x_0/\partial y'$, $\dot\sigma = \partial\sigma/\partial y'$, and the metric tensor of the transformation $\boldsymbol{g}$ is equal to

$$\boldsymbol{g} = \left(\frac{\partial \boldsymbol{x}}{\partial \boldsymbol{x}'}\right)^{\mathrm{T}} \cdot \left(\frac{\partial \boldsymbol{x}}{\partial \boldsymbol{x}'}\right) = \begin{pmatrix} \sigma^2 & \sigma(\dot\sigma x'+\dot x_0) \\ \sigma(\dot\sigma x'+\dot x_0) & 1+(\dot\sigma x'+\dot x_0)^2 \end{pmatrix}. \tag{20}$$

The out-of-plane components are $\epsilon_{zz} = \sqrt{g}\epsilon$ and $\mu_{zz} = \sqrt{g}$. Therefore, a corollary of the above results is that there are *planar* profiles that are inhomogeneous, anisotropic, and complex and are reflectionless. This is irrespective of the fact that these anisotropic media are inhomogeneous in both x' and y' coordinates.

IV. CONCLUSION

Reflectionless potentials represent an important class of scatteringless systems in classical and quantum physics. Such potentials, originally introduced in some pioneering works by Pöschl and Teller [2] and Kay and Moses [1], play a major role in the theory of solitons in nonlinear physics and in supersymmetric theory of quantum mechanics. Reflectionless potentials are commonly introduced in the framework of Hermitian systems, where inverse scattering methods provide powerful means to synthesize, with a surprising amount of freedom, transparent potentials with an arbitrary number of independent parameters. Recently, great interest has been devoted to the synthesis and experimental realization of reflectionless potentials that are *non-Hermitian* [11–20]. Non-Hermitian potentials include regions of space where the wave is locally either amplified or absorbed and this opens up new ways to control wave scattering. For instance, to transmit without backscattering, a lossless potential must guide the wave energy around an object, whereas a non-Hermitian potential may absorb the energy on one side, putting it back on the other. In addition, in comparison to Hermitian reflectionless potentials, non-Hermitian ones generally show a different behavior, for example, they can be reflectionless only *unidirectionally*, thus opening up new ways to control and engineer wave scattering.

In this work we have disclosed an important property of reflectionless non-Hermitian potentials, which is not shared by their Hermitian counterparts, namely, their robustness to deformation in space or time. Specifically, we have shown that the class of non-Hermitian potentials with a profile satisfying the spatial Kramers-Kronig relations [20] remain reflectionless after certain space or time deformation. The physical mechanism underlying this property is very similar to that explained in [20]: The potential is made up of only positive Fourier components (and is thus necessarily complex valued) and so is unable to reduce the momentum of a right propagating wave, whatever order of scattering process we consider. This property is not disturbed by the motion of the potential or for certain deformations of the potential in space. We have demonstrated this by considering, as the simplest case, scattering of matter waves from an arbitrarily moving Kramers-Kronig potential. We have then extended our analysis to electromagnetic waves by considering wave scattering from a deformed slab of reflectionless dielectric material. Using conformal mapping methods, a rather broad class of spatial deformation, including the case where the potential is both scaled and has its center displaced as an arbitrary function of position, has been introduced. Numerical simulations corroborate the analytical theory and demonstrate that the backscattering from these deformed profiles remains zero, even for extreme deformations.

At this point we should emphasize that while the potentials remain reflectionless after being deformed in space or time, the other scattering characteristics do change. For example, if we consider a rapidly oscillating potential (using the theory developed in Sec. II), then to leading order the wave will experience a time-averaged potential $V_{\mathrm{eff}}(x) = T^{-1}\int_0^T dt\, V(x - x_0(t))$ (T the modulation period). We can immediately see that if $V(x)$ is a Kramers-Kronig potential, then so is $V_{\mathrm{eff}}(x)$, guaranteeing zero backscattering for incidence from one side. However, the shape of the two potentials is different, meaning that the remaining scattering characteristics such as the transmission and the scattering for incidence from the other side will be different.

Our results suggest the supremacy of non-Hermitian Kramers-Kronig potentials over their Hermitian counterparts, providing a new route toward wave scattering control and engineer with potential applications to, e.g., reflectionless optical coatings for surfaces with sharp edges [28].

ACKNOWLEDGMENTS

S.A.R.H. acknowledges financial support through a Royal Society TATA University Research Fellowship (Grant No. RPG-2016-186).

[1] I. Kay and H. E. Moses, Reflectionless transmission through dielectrics and scattering potentials, J. Appl. Phys. **27**, 1503 (1956).

[2] G. Pöschl and E. Teller, Bemerkungen zur quantenmechanik des anharmonischen oszillators, Z. Phys. **83**, 143 (1933).

[3] J. Lekner, Reflectionless eigenstates of the sech^2 potential, Am. J. Phys. **75**, 1151 (2007).

[4] T.-Y. Wu and T. Ohmura, *Quantum Theory of Scattering* (Dover, New York, 2011).

[5] P. G. Drazin and R. S. Johnson, *Solitons* (Cambridge University Press, Cambridge, 1989).

[6] C. V. Sukumar, Supersymmetry, potentials with bound states at arbitrary energies and multi-soliton configurations, J. Phys. A **19**, 2297 (1986).

[7] P. Borys, F. Garcia-Sanchez, J.-V. Kim, and R. L. Stamps, Spin-wave eigenmodes of Dzyaloshinskii domain walls, Adv. Electron. Mater. **2**, 1500202 (2016).

[8] N. Moiseyev, *Non-Hermitian Quantum Mechanics* (Cambridge University Press, Cambridge, 2011).

[9] C. M. Bender and S. Boettcher, Real Spectra in Non-Hermitian Hamiltonians Having $\mathcal{PT}$ Symmetry, Phys. Rev. Lett. **80**, 5243 (1998).

[10] C. M. Bender, Making sense of non-Hermitian Hamiltonians, Rep. Prog. Phys. **70**, 947 (2007).

[11] Z. Ahmed, C. M. Bender, and M. V. Berry, Reflectionless potentials and $\mathcal{PT}$ symmetry, J. Phys. A **38**, L627 (2005).

[12] Z. Lin, H. Ramezani, T. Eichelkraut, T. Kottos, H. Cao, and D. N. Christodoulides, Unidirectional Invisibility Induced by $\mathcal{PT}$-Symmetric Periodic Structures, Phys. Rev. Lett. **106**, 213901 (2011).

[13] S. Longhi, Invisibility in $\mathcal{PT}$-symmetric complex crystals, J. Phys. A **44**, 485302 (2011).

[14] A. Mostafazadeh, Invisibility and $\mathcal{PT}$ symmetry, Phys. Rev. A **87**, 012103 (2013).

[15] X. Zhu, H. Ramezani, C. Shi, J. Zhu, and X. Zhang, $\mathcal{PT}$-Symmetric Acoustics, Phys. Rev. X **4**, 031042 (2014).

[16] R. Fleury, D. Sounas, and A. Alù, An invisible acoustic sensor based on parity-time symmetry, Nat. Commun. **6**, 5905 (2015).

[17] A. Regensburger, C. Bersch, M.-A. Miri, G. Onishchukov, D. N. Christodoulides, and U. Peschel, Parity-time synthetic photonic lattices, Nature (London) **488**, 167 (2012).

[18] L. Feng, Y.-L. Xu, W. S. Fegadolli, M.-H. Lu, J. E. B. Oliveira, V. R. Almeida, Y.-F. Chen, and A. Scherer, Experimental demonstration of a unidirectional reflectionless parity-time metamaterial at optical frequencies, Nat. Mater. **12**, 108 (2013).

[19] C. Shi, M. Dubois, Y. Chen, L. Cheng, H. Ramezani, Y. Wang, and X. Zhang, Accessing the exceptional points of parity-time symmetric acoustics, Nat. Commun. **7**, 11110 (2016).

[20] S. A. R. Horsley, M. Artoni, and G. C. La Rocca, Spatial Kramers-Kronig relations and the reflection of waves, Nat. Photon. **9**, 436 (2015).

[21] S. Longhi, Wave reflection in dielectric media obeying spatial Kramers-Kronig relations, Europhys. Lett. **112**, 64001 (2016).

[22] S. A. R. Horsley, C. G. King, and T. G. Philbin, Wave propagation in complex coordinates, J. Opt. **18**, 044016 (2016).

[23] S. A. R. Horsley, The KdV hierarchy in optics, J. Opt. **18**, 085104 (2016).

[24] G. W. Milton, Analytic materials, Proc. R. Soc. A **472**, 20160613 (2016).

[25] M. V. Berry, Lop-sided diffraction by absorbing crystals, J. Phys. A **31**, 3493 (1998).

[26] G. W. Milton, Exact band structure for the scalar wave equation with periodic complex moduli, Physica B **338**, 186 (2003).

[27] S. Longhi, Bidirectional invisibility in Kramers-Kronig optical media, Opt. Lett. **41**, 3727 (2016).

[28] W. Jiang, Y. Ma, J. Yuan, G. Yin, W. Wu, and S. He, Deformable broadband metamaterial absorbers engineered with an analytical spatial Kramers-Kronig permittivity profile, Laser Photon. Rev. **11**, 1600253 (2017).

[29] M. Gavrila, Atomic stabilization in superintense laser fields, J. Phys. B **35**, R147 (2002).

[30] M. Pont, N. R. Walet, M. Gavrila, and C. W. McCurdy, Dichotomy of the Hydrogen Atom in Superintense, High-Frequency Laser Fields, Phys. Rev. Lett. **61**, 939 (1988).

[31] M. Pont and M. Gavrila, Stabilization of Atomic Hydrogen in Superintense, High-Frequency Laser Fields of Circular Polarization, Phys. Rev. Lett. **65**, 2362 (1990).

[32] F. Morales, M. Richter, S. Patchkovskii, and O. Smirnova, Imaging the Kramers-Henneberger atom, Proc. Natl. Acad. Sci. USA **108**, 16906 (2011).

[33] K. W. Madison, C. F. Bharucha, P. R. Morrow, S. R. Wilkinson, Q. Niu, B. Sundaram, and M. G. Raizen, Quantum transport of ultracold atoms in an accelerating optical potential, Appl. Phys. B **65**, 693 (1997).

[34] S. Longhi, Quantum-optical analogies using photonic structures, Laser Photon. Rev. **3**, 243 (2009).

[35] S. Longhi, M. Marangoni, D. Janner, R. Ramponi, P. Laporta, E. Cianci, and V. Foglietti, Observation of Wave Packet Dichotomy and Adiabatic Stabilization in an Optical Waveguide, Phys. Rev. Lett. **94**, 073002 (2005).

[36] I. Vorobeichik, R. Lefebvre, and N. Moiseyev, Field-induced barrier transparency, Europhys. Lett. **41**, 111 (1998).

[37] S. Longhi, Resonant tunneling in frustrated total internal reflection, Opt. Lett. **30**, 2781 (2005).

[38] F. J. Flanigan, *Complex Variables* (Dover, New York, 1983).

[39] H. Cartan, *Elementary Theory of Analytic Functions of One or Several Complex Variables* (Dover, New York, 1995).

[40] J. B. Pendry, D. Schurig, and D. R. Smith, Controlling electromagnetic fields, Science **312**, 1780 (2006).

[41] U. Leonhardt and T. G. Philbin, *Geometry and Light: The Science of Invisibility* (Dover, New York, 2010).